Dynamical Masses of Elliptical Galaxies

Ortwin Gerhard

Astronomisches Institut, Universität Basel, Venusstrasse 7, 4102 Binningen, Switzerland

Abstract. Recent progress in the dynamical analysis of elliptical galaxy kinematics is reviewed. Results reported briefly include (i) the surprisingly uniform anisotropy structure of luminous ellipticals, (ii) their nearly flat (to $\sim 2R_e$) circular velocity curves, (iii) the Tully-Fisher and $M/L - L$ relations and the connection to the Fundamental Plane, and (iv) the large halo mass densities implied by the dynamical models.

1 Introduction

Elliptical galaxies are the most massive galaxies and are generally found in dense environments. In the context of hierarchical models, they represent an advanced step in the galaxy formation process. Their mass distributions and dark halo properties, while not yet as well-understood observationally as those of spiral galaxies, are of considerable interest. X-ray and gravitational lensing studies imply mass-to-light ratios $M/L \sim 100$ on scales of ~ 100 kpc for the most massive ellipticals containing hot gas atmospheres. Here the new XMM and Chandra satellite data will lead to mass measurements of unprecedented resolution and accuracy.

In the central $\sim 2R_e$, mass distributions $M(r)$ may be determined from absorption-line profile measurements and dynamical models. Planetary nebulae and globular clusters can be used as discrete velocity tracers to $\sim 4-5R_e$ (typical effective radii R_e are in the range 3-10 kpc). In less massive, gas-poor systems these may give the main constraints on $M(r)$. In gas-rich ellipticals where $M(r)$ can be accurately determined from the X-ray gas emission, the stellar-kinematic data will constrain the orbit structure best.

The following sections give a brief review of the dynamical analysis of the stellar-kinematic data, and the results obtained so far on mass distributions in ellipticals and on their dynamical family properties.

2 Dynamical mass estimation

As is well known, velocity dispersion profile measurements (and streaming velocities, if the galaxy rotates) do not suffice to determine the distribution of mass with radius, due to the degeneracy with orbital anisotropy. Only with very extended measurements can a constant M/L model be ruled out (e.g., Saglia *et al.* 1993), but even then the detailed $M(r)$ remains undetermined. Absorption line profile shapes (giving line-of-sight velocity distributions $L(v)$, LOSVD

for short), however, contain additional information with which this degeneracy can largely be broken. Simple spherical models are useful to illustrate this (Gerhard 1993): at large radii, radial orbits are seen side-on, resulting in a peaked LOSVD (positive Gauss-Hermite parameter h_4), while tangential orbits lead to a flat-topped or double-humped LOSVD ($h_4 < 0$). Similar considerations can be made for edge-on or face-on disks (Bender 1990, Magorrian & Ballantyne 2001) and spheroidal systems (Dehnen & Gerhard 1993).

One may think of the LOSVDs constraining the anisotropy, after which the Jeans equations can be used to determine the mass distribution. However, the gravitational potential influences not only the widths, but also the shapes of the LOSVDs (see illustrations in Gerhard 1993). Furthermore, eccentric orbits visit a range of galactic radii and may therefore broaden a LOSVD near their pericentres as well as leading to outer peaked profiles. Thus, in practise, the dynamical modelling to determine the orbital anisotropy and gravitational potential must be done globally, and is typically done in the following steps:

(0) choose geometry (spherical, axisymmetric, triaxial);

(1) choose dark halo model parameters, and set total luminous plus dark matter potential Φ;

(2) write down a composite distribution function (DF) $f = \Sigma_k a_k f_k$, where the f_k can be orbits, or DF components such as $f_k(E, L^2)$, with free a_k;

(3) project the f_k to observed space, $p_{jk} = \int K_j f_k d\tau$, where K_j is the projection operator for observable P_j, and τ denotes the line-of-sight coordinate and the velocities;

(4) fit the data $P_j = \Sigma_k a_k p_{jk}$ for all observables P_j simultaneously, minimizing a χ^2 or negative likelihood, and including regularization to avoid spurious large fluctuations in the solution. This determines the a_k, i.e, the best DF f, given Φ, which must be $f > 0$ everywhere;

(5) vary Φ, go back to (1), and determine confidence limits on the parameters of Φ.

Such a scheme was employed, e.g., using orbits in spherical potentials by Rix *et al.* (1997) and Romanowsky & Kochanek (2001); using DF components in spherical potentials by Gerhard *et al.* (1998), Saglia *et al.* (2000), and Kronawitter *et al.* (2000); with orbits in axisymmetric geometry by Cretton *et al.* (2000) and Gebhardt *et al.* (2000); and with DF components in axisymmetry by Matthias & Gerhard (1999) and Statler *et al.* (1999). The modelling techniques used to constrain black hole masses from nuclear kinematics and dark halo parameters from extended kinematics are very similar.

Line-profile shape parameter measurements are now available for many nearby ellipticals (e.g., Bender, Saglia & Gerhard 1994), but those reaching to $\sim 2R_e$ are still scarce (see Kronawitter *et al.* 2000). Modelling of the mass profiles of ellipticals from such data has been done for some two dozen round galaxies in the spherical approximation, and for a few cases using axisymmetric three-integral models.

Typically the models that fit individual galaxies best imply small to modest amounts of dark matter within $2R_e$, but there are ellipticals which are very well

represented by constant M/L models out to these radii. Most results obtained so far are from spherical models for round ellipticals; their mass distributions and radially anisotropic orbit structure are discussed in the next section. The effects of intrinsic deviations from sphericity and of embedded, near-face-on disks have been discussed by Kronawitter *et al.* (2000), Magorrian & Ballantyne (2001), and Gerhard *et al.* (2001). Axisymmetric models exist only for very few ellipticals. In NGC 1600 (E3.5, Matthias & Gerhard 1999), NGC 2300 (E2, Kaeppeli 1999), NGC 2320 (E3.5, Cretton, Rix & de Zeeuw 2000), and NGC 3379 (E1, Gebhardt *et al.* 2000) radially anisotropic structure at $\sim 0.5R_e$ has been inferred from three-integral models along the major axis, similar to that found in the round galaxies, but with less anisotropy on the minor axis.

Because the dark matter fraction inside $2R_e$ is still modest, and the orbit structure in the outer main bodies of ellipticals is not well-constrained by data that end at $2R_e$, it will be important to include discrete velocity data from planetary nebulae (PN) or globular clusters (GC) that reach to larger radii. Such data can be included directly in the above modelling scheme, using a likelihood maximization (Romanowsky & Kochanek 2001), or can be used a posteriori to differentiate between dynamical models at radii beyond the absorption line data on which these are based (Saglia *et al.* 2000). The number of ellipticals with such data is still small, but is expected to be growing rapidly thanks to the special purpose PN spectrograph (Douglas *et al.* 2002) and ongoing programs with globular cluster samples around ellipticals. Typically one may expect a few hundred discrete velocities per galaxy from these programs. Using slitless spectroscopy at the VLT Méndez *et al.* (2001) succeeded in measuring 535 PN radial velocities around the E5 galaxy NGC 4697. Detailed modelling of these data is still in progress, but simple models for this relatively low luminosity elliptical galaxy are consistent with constant M/L out to $\sim 3R_e$, in agreement with Dejonghe *et al.* (1996).

Two particularly interesting cases are the central galaxies of the Fornax and Virgo clusters, NGC 1399 and M87. From a comparison of dynamical models for the absorption line kinematics (Saglia *et al.* 2000) with the mass distribution obtained from ASCA data (Ikebe *et al.* 1996), it appears that PN (Arnaboldi *et al.* 1994) and GC velocities (Richtler *et al.* 2001) are just in the right radial range to allow a study of the transition between the potential of the central NGC 1399 galaxy and the potential of the Fornax cluster. Similarly, from a study of the stellar kinematics and the GC velocities around M87, and a comparison to the X-ray mass profile, Romanoswky & Kochanek (2001) find a rising circular velocity curve, and suggest that the potential of the Virgo cluster may already dominate at $r \sim 20\,\mathrm{kpc}$ from the center of M87.

3   Dynamical family properties

The discussion in this section is based on the work of Kronawitter *et al.* (2000) and Gerhard *et al.* (2001), who analyzed the line-profile shapes of a sample of 21 mostly luminous, slowly rotating, and nearly round elliptical galaxies in

a uniform way, using spherical dynamical models. A similar study using three-integral axisymmetric models will be very worthwhile, but is still some time away. The sample of Kronawitter *et al.* includes a subsample with mostly new extended kinematic data, reaching to $\sim 2R_e$, and a subsample based on the less extended older data of Bender *et al.* (1994). Based on these data and on photometry, non-parametric spherical models were constructed from which circular velocity curves, anisotropy profiles, and radial profiles of M/L were derived, including confidence ranges. The main results from this study are as follows.
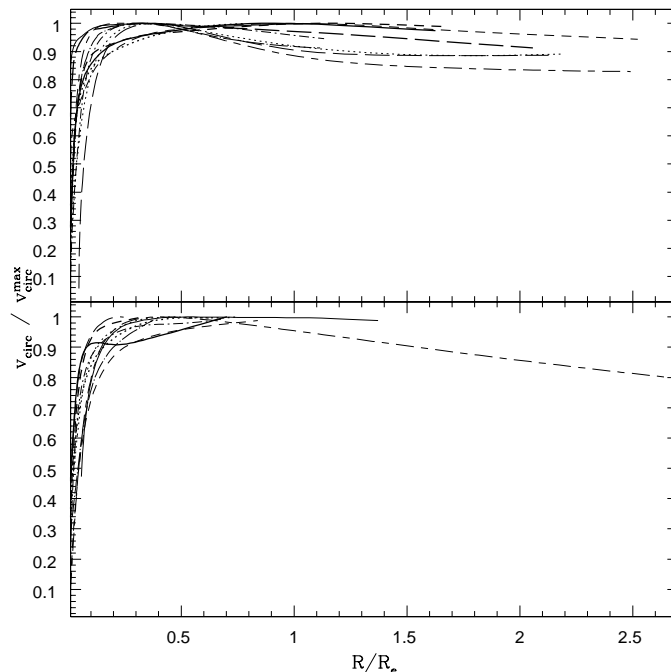
(1) The circular velocity curves (CVCs) of elliptical galaxies are flat to within $\simeq 10\%$ for $R \gtrsim 0.2R_e$ to at least $R \gtrsim 2R_e$, independent of luminosity (Fig. 1). The CVC is a convenient measure of the potential even though luminous elliptical galaxies do not rotate rapidly. Quantitatively, the median ratio of the circular velocity at the radius of the outermost kinematic data point, $v_c(R_{\max})$, to the maximum circular velocity of the respective best model, $v_c^{\max}$, is 0.94, with 95% confidence ranges of $\sim \pm 0.1$. This argues against strong luminosity segregation in the dark halo potential.

(2) Despite the uniformly flat CVCs, there is a spread in the ratio of the CVCs from luminous and dark matter, i.e., in the radial variations of cumulative mass-to-light ratio. The sample includes galaxies with no indication for dark matter within $2R_e$, and others where the best dynamical models result in local M/L_Bs of 20-30 at $2R_e$. As in spiral galaxies, the combined rotation curve of the luminous and dark matter is flatter than those for the individual components ("conspiracy").

(3) Most of these ellipticals are moderately radially anisotropic, with average $\beta \equiv 1 - \sigma_\theta^2/\sigma_r^2 \simeq 0 - 0.35$, again independent of luminosity. The dynamical structure of ellipticals is therefore surprisingly uniform. The maximum circular velocity is accurately predicted by a suitably defined central velocity dispersion. Averaging σ within $0.1R_e$, $\sigma_{0.1} = 0.66v_c^{\max}$.

(4) Elliptical galaxies follow a Tully-Fisher (TF) relation with marginally shallower slope than spiral galaxies (see also Magorrian & Ballantyne 2001). At given circular velocity, they are about 1 mag fainter in B and about 0.6 mag in R, and appear to have slightly lower baryonic mass than spirals, even for the maximum M/L_B allowed by their kinematics (minimum dark halo models). The residuals from the TF (and Fundamental Plane, FP) relations do not correlate with dynamical anisotropy β.

(5) The luminosity dependence of M/L_B indicated by the tilt of the FP corresponds to a real dependence of dynamical M/L_B on L_B. The tilt of the FP is therefore not due to deviations from homology or a variation of dynamical anisotropy with L_B, although the slope of M/L_B versus L_B could still be influenced by photometric non-homology. The tilt can also not be due to an increasing dark matter fraction with L_B, unless (i) the most luminous ellipticals have a factor > 3 less baryonic mass than spiral galaxies of the same circular velocity, and (ii) the range of IMF is larger than currently discussed, and (iii) the IMF or some other population parameter varies systematically along the luminosity sequence such as to undo the increase of M/L_B expected from sim-

Fig. 1. "Best model" circular velocity curves of all galaxies from the Kronawitter *et al.* (2000) sample, plotted as a function of radius scaled by the effective radius R_e, and normalized by the maximum circular velocity. The upper panel shows the galaxies from the extended kinematics subsample, the lower panel the galaxies from the subsample with older data from Bender *et al.* (1994). From Gerhard *et al.* (2001).

ple stellar population models for more metal-rich luminous galaxies. This seems highly unlikely.

(6) The tilt of the FP is therefore best explained as a stellar population effect. Population models show that the values and the change with L_B of the maximal dynamical M/L_Bs are consistent with the stellar population M/L_Bs based on published metallicities and ages, within the uncertainties of IMF and distance scale. Because of (5) above and because the observed correlation between age and luminosity is far too weak to explain the $M/L_B - L_B$ relation (Forbes & Ponman 1999), the main driver of the B-band tilt is therefore probably metallicity. This would not explain the observed K-band tilt, which must then be explained by a secondary population effect.

(7) The population models show that the dynamical models would have overestimated the luminous masses of these elliptical galaxies by as much as a factor ≈ 2 only if (i) the flattest IMFs at low stellar masses discussed for the Milky Way are applicable, and simultaneously (ii) a short distance scale

$(H_0 \simeq 80\,\mathrm{km\,s^{-1}\,Mpc^{-1}})$ turns out to be correct. For lower values of H_0 and/or other IMFs the difference is smaller. Together with (4) this makes it likely that elliptical galaxies have indeed nearly maximal M/L_B ratios (minimal halos).

(8) In the models with maximum stellar mass, the dark matter contributes $\sim 10 - 40\%$ of the mass within R_e. The flat CVC models, when extrapolated beyond the range of kinematic data, predict equal interior mass of dark and luminous matter at $\sim 2 - 4R_e$, consistent with results from X-ray analyses.

(9) Even in maximum stellar mass models, the halo core densities and phase-space densities are at least ~ 25 times larger and the halo core radii ~ 4 times smaller than in maximum disk spiral galaxies with the same circular velocity (Persic, Salucci & Stel 1996). Correspondingly, the increase in M/L sets in at ~ 10 times larger acceleration than in spirals. This could imply that elliptical galaxy halos collapsed at high redshifts or perhaps even that some of the dark matter in ellipticals might be baryonic.

References

1. Arnaboldi, M., Freeman, K.C., Hui, X., Capaccioli, M., Ford, H., 1994, The Messenger, 76, 40
2. Bender, R., 1990, A&A, 229, 441
3. Bender, R., Saglia, R.P., Gerhard, O., 1994, MNRAS, 269, 785
4. Cretton, N., Rix, H.-W., de Zeeuw, T., 2000, ApJ, 536, 319
5. Dehnen, W., Gerhard, O.E., 1993, MNRAS, 261, 311
6. Dejonghe, H., De Bruyne, V., Vauterin, P., Zeilinger, W.W., 1996, A&A, 306, 363
7. Douglas, N.G., et al., 2002, PASP, submitted
8. Forbes, D.A., Ponman, T.J., 1999, MNRAS, 309, 623
9. Gebhardt, K., etal, 2000, AJ, 119, 1157
10. Gerhard, O.E., 1993, MNRAS, 265, 213
11. Gerhard, O.E., Jeske, G., Saglia, R.P., Bender, R., 1998, MNRAS, 295, 197
12. Gerhard, O.E., Kronawitter, A., Saglia, R.P., Bender, R., 2001, AJ, 121, 1936
13. Ikebe, Y., et al., 1996, Nature, 379, 427
14. Kaeppeli, A., 1999, Diploma Thesis, Univ. of Basel
15. Kronawitter, A., Saglia, R.P., Gerhard, O.E., Bender, R., 2000, A&AS, 144, 53
16. Magorrian, J., Ballantyne, D., 2001, MNRAS, 322, 702
17. Matthias, M., Gerhard, O.E., 1999, MNRAS 310, 879
18. Méndez, R.H., et al., 2001, ApJ, 563, 135
19. Persic, M., Salucci, P., Stel, F., 1996, MNRAS, 281, 27
20. Richtler, T., et al., 2001, in 'Extragalactic star clusters', IAU Symp. 207, ed. E.K. Grebel et al., ASP, in press
21. Rix, H.-W., de Zeeuw, P.T., Cretton, N., van der Marel, R., Carollo, C.M., 1997, ApJ, 488, 702
22. Romanowsky, A.J., Kochanek, C.S., 2001, ApJ, 553, 722
23. Saglia, R.P., et al., 1993, ApJ, 403, 567
24. Saglia, R.P., Kronawitter, A., Gerhard, O.E., Bender, R., 2000, AJ, 119, 153
25. Statler, T.S., Dejonghe, H., Smecker-Hane, T., 1999, ApJ, 117, 126